Neutron diffraction studies on a ferromagnetic layered manganite $La_{2-2x}Sr_{1+2x}Mn_2O_7$ ($x=0.3$) prepared by a ceramic method

Eun-Ok Chi, Kun-Pyo Hong, and Young-Uk Kwon
Department of Chemistry, Sungkyunkwan University, Suwon 440-746, Korea

N. P. Raju and John E. Greedan
Brockhouse Institute for Materials Research and Department of Chemistry, McMaster University, Hamilton, Ontario, Canada L8S 4M1

Jeong-Soo Lee
Korea Atomic Energy Research Institute, Taejon 305-600, Korea

Nam Hwi Hur
Korea Research Institute of Science and Standards, Taejon 306-600, Korea
(Received 24 May 1999)

Low-temperature neutron diffraction data on a ceramic sample of layered perovskite type $La_{2-2x}Sr_{1+2x}Mn_2O_7$, $x=0.3$, are reported. The neutron diffraction data show that this compound undergoes a ferromagnetic transition at 100 K (T_c), but there is no antiferromagnetic signal as reported on a floating zone melt grown sample of the same nominal composition. The unit cell constants and cell volume for this nominal $x=0.3$ sample are slightly larger than those for samples which do show an antiferromagnetic component which indicates a higher Sr content. The magnetic structure was determined to have colinear Mn spins with a tilting angle against the *c* axis. The tilting angle abruptly increases from about 20° near T_c to about 50° at 75 K and then gradually decreases afterwards to 30° at 15 K. This anomalous tilting angle behavior correlates with a distortion index based on the variance of the Mn-O bond distances and can be understood qualitatively with a simple crystal field argument. Below T_c, there is a magnetostrictive effect on the *c* axis which correlates with the behaviors of the spin orientation and the Mn-O bond distances. [S0163-1829(99)08241-7]

INTRODUCTION

Since the discovery of the strongly anisotropic colossal magnetoresistance (CMR) and other physical properties of layered $n=2$ Ruddlesden-Popper (RP) phases, $La_{2-2x}Sr_{1+2x}Mn_2O_7$ ($x=0.3$ and 0.4) (Fig. 1), there has been much effort to understand the nature of these materials.[1–14] The physical properties of these compounds show a strong dependence on the hole doping level (x). For example, for the $x=0.4$ compound is reported that both ρ_{ab} and ρ_c show metal-to-nonmetal transitions with concomitant ferromagnetic (FM) transitions at 120 K,[1] while the $x=0.3$ compound is reported to have two different transition temperatures at 100 and 260 K.[2] The higher-temperature transition was attributed to the onset of a two-dimensional (2D) double-exchange interaction and the lower to the 3D ordering of the 2D metallic and FM layers.[4–8] However, there has been controversy on the existence[9] and the nature[6–8] of the 2D FM state of this compound.

Recently, employing low-temperature neutron diffraction, Perring *et al.*[10] and Argyriou *et al.*[11] showed that their float zone melt grown $x=0.3$ samples had interbilayer antiferromagnetic (AF) interactions. They argued that this AF interaction is responsible for the large MR along the *c* direction reported by Kimura *et al.*[2] Argyriou *et al.* also reported that their sample had a FM minor $n=2$ RP phase. The lattice parameters of this minor phase, with respect to the major one, indicated that it had a larger *x*. Indeed, such an AF interbilayer interaction is not reported for the $x=0.4$ compound.[12,13]

Noting that the physical properties of these layered compounds are very sensitive to the doping level, we have started a systematic study by varying *x*. Especially, we have em-

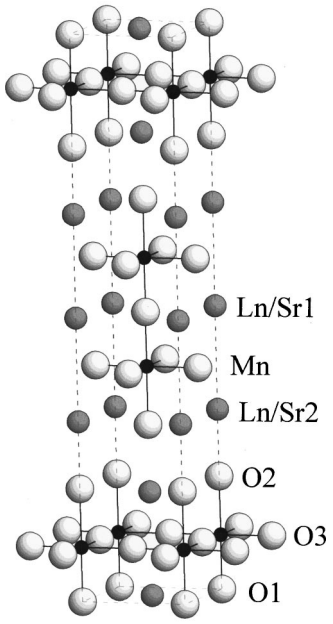

FIG. 1. Structure and labeling scheme for $La_{2-2x}Sr_{1+2x}Mn_2O_7$ compounds.

ployed the solid-state synthesis method, which may provide a point of comparison with the literature samples that are mostly prepared by the float zone melting technique.

In this paper, we present our low-temperature neutron diffraction data on a ceramic $x=0.3$ sample. We show that our sample does not have any AF component, but is composed of a pure FM phase in which the Mn moments are tilted with respect to the *c* axis. In addition, the refinement results show that there is an anomalous behavior of the temperature dependence of the tilt angle.

EXPERIMENT

About 7 g of a polycrystalline $La_{2-2x}Sr_{1-2x}Mn_2O_7$, $x=0.3$, sample was prepared according to our previous paper.[14] Stoichiometric amounts of La_2O_3 (heated at 700 °C prior to use), $SrCO_3$, and Mn_2O_3 were ground together, pressed into a pellet, and heated at 1400 °C for total of 100 h with several cycles of intermittent grinding, pelletizing, and heating to ensure a single-phase product.

Field-dependent magnetization data at 300 K obtained with a superconducting quantum interference device (SQUID) magnetometer indicate that there is a ferromagnetic impurity which was identified as a perovskite phase of composition close to $La_{0.6}Sr_{0.4}MnO_3$ based on a neutron diffraction data analysis.[15] The temperature-dependent resistivity and magnetic susceptibility data show that this compound undergoes a transition from a paramagnetic insulator to a ferromagnetic metal at 100 K.[14]

Powder x-ray diffraction data for Rietveld profile refinement were recorded on a Nicolet 12 diffractometer using Cu $K\alpha$ radiation in the 2θ range 10°–90° with a step size of 0.03° and a counting period of 21 s per step.

Neutron powder diffraction data at various temperatures were obtained on a HRPD at HANARO Center, KAERI, Korea, using 1.8339 Å neutrons obtained by reflection from a single-crystal Ge (331) monochromator. The sample was loaded in a V can ($\phi=8$ mm, $L=80$ mm), which, in turn, was placed in a He-filled Al canister for the low-temperature experiments. The temperature of the sample was monitored at the top and bottom of the V can to ensure thermal homogeneity of the sample.

The Rietveld profile refinements were performed by using the FULLPROF (Ref. 16) and GSAS (Ref. 17) programs. Five parameters of Chevynev-type background parameters, pseudo-Voigt-type profile function with three parameters, and asymmetric peak shape function with four terms were used in the refinements with FULLPROF. For the refinements with GSAS, the background was refined with a 12-term cosine Fourier series, and the peak profile was refined with a pseudo-Voigt function with eight terms.

RESULTS AND DISCUSSION

Both the room-temperature powder neutron and x-ray diffraction patterns of our sample were refined simultaneously to get the parameters in Table I. X-ray data can be used to differentiate La and Sr, and thus the distribution of these ions over the two possible sites (rocksalt and perovskite sites) could be determined. The results are that 49(3)% of the total La occupies the rocksalt site, which is smaller than a random distribution, 66.7%. A similar behavior of the Sr and La distributions was also found in the other $La_{2-2x}Sr_{1+2x}Mn_2O_7$ compounds with different hole doping levels ($x=0.4$ and 0.5) and can be attributed to the matching between the average size of La/Sr and the perovskite hole size provided by the rather rigid Mn-O framework.[18,19]

TABLE I. Simulations refinement results of powder x-ray and neutron diffraction data for $La_{2-2x}Sr_{1+2x}Mn_2O_7$, $x=0.3$, at room temperature. $a=3.868\,66(9)$ Å, $c=20.3066(7)$ Å, and $V=303.92(2)$ Å^3. For x-ray data $wRp=11.81$, $Rp=9.29$, fraction of the major phase=94.485%. For neutron data $wRp=11.52$, $Rp=8.85$, fraction of the major phase=90.319%. The total is $wRp=11.61$, $Rp=8.98$, and $\chi^2=3.086$.

	z	U_{iso} (Å^2)	Occupancy
O(1)	0	0.017(2)	1
O(2)	0.1960(2)	0.012(2)	1
O(3)	0.0954(1)	0.082(8)	1
La(1)	0.5	0.003(1)	0.71(4)
Sr(1)	0.5	0.003(1)	0.29(4)
La(2)	0.3168(1)	0.004(1)	0.34(2)
Sr(2)	0.3168(1)	0.004(1)	0.66(2)
Mn	0.0965(3)	0.0009(11)	1
Mn-O(1)	1.959(6) Å		
Mn-O(2)	2.021(8) Å		
Mn-O(3)	1.93445(9)Å		
O(1)-Mn-O(3)	89.36(19) Å		
O(3)-Mn-O(3)	178.7(4) Å		

The lattice parameters of our sample from this refinement [$a=3.86866(9)$ Å, $c=20.3066(7)$ Å] are close to those the other nominal $x=0.3$ compounds reported in the literature. Lattice parameters can be a good indicator of the doping level *x* of this system. From a systematic study of the crystal structures of $La_{2-2x}Sr_{1-2x}Mn_2O_7$, Seshadri *et al.* determined that the lattice parameters show the following dependence on *x*:[20]

$$a=3.8440(6)+0.0726(10)x,$$

$$c=20.864(6)-1.832(10)x.$$

According to these equations, the *x* value of our compound is 0.340 and 0.304 based on the *a* and *c* parameters, respectively. The lattice parameters of the sample of Argyriou *et al.*[11] convert to $x=0.245$ (for the *a* parameter) and 0.278 (for the *c* parameter). Of course, these results cannot be taken as an absolute measure, but still may be useful in comparing the relative composition. The utility of the above formulas can be confirmed from a calculation on an $x=0.4$ compound reported by Mitchell *et al.* which gives *x* values of 0.417 and 0.392 based on *a* and *c* parameters, respectively.[12] It is clear that our $x=0.3$ sample is richer in Sr than that of Ref. 11, but the difference is fairly small.

The x-ray powder diffraction pattern of our compound did not reveal any sign of the biphasic nature reported for the related $LSr_2Mn_2O_7$ (L=La–Gd) (Ref. 18) and $Nd_{2-2x}Sr_{1+2x}Mn_2O_7$ ($x=0.4$ and 0.45) (Refs. 21 and 22) compounds. According to Battle *et al.*, many samples of the $n=2$ members of the RP manganites may be composed of

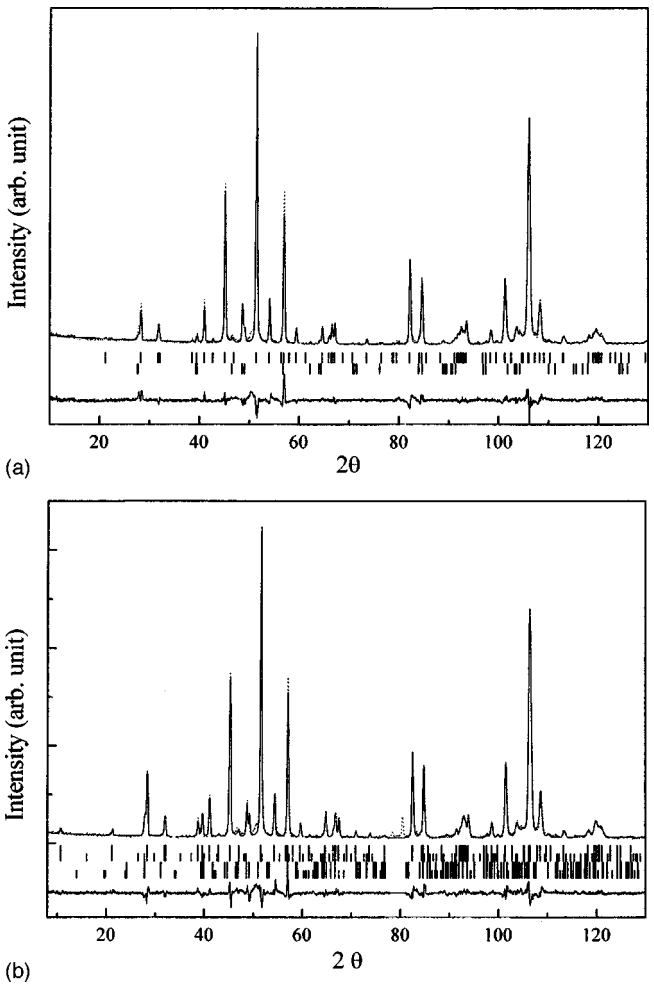

FIG. 2. Calculated and observed powder neutron diffraction patterns for $La_{2-2x}Sr_{1+2x}Mn_2O_7$, $x=0.3$, at room temperature (a) and 15 K (b).

two phases with slightly different lattice parameters.[18] They argued that the two-phase nature is apparent from the peak shape of the (0 0 10) reflection, the profile fitting with a biphasic model giving much better agreement than a single-phase model. A similar result was reported for the $x=0.3$ sample by Argyriou *et al.* who employed synchrotron x-ray diffraction to resolve the two-phase nature of their sample. Based on their magnetic neutron diffraction data, they concluded that the major phase had an AF interbilayer interaction while the minor was FM. However, their neutron diffraction patterns did not reveal the two-phase mixing because of the lower resolution of the neutron diffractometer.[11] In attempts to fit the x-ray diffraction data for our nominal $x=0.3$ sample with a biphasic model with and without constraints, we have obtained merging lattice parameters or divergent results. Our inability to observe two-phase mixing in our sample is not conclusive and may be due to the lower resolution of the laboratory x-ray system which uses Cu $K\alpha$ radiation. However, the magnetic neutron diffraction data at low temperatures (below) were refined successfully with a single $n=2$ RP phase model (plus a perovskite impurity) as also reported in Ref. 11.

The neutron diffraction patterns of our sample show that there is a perovskite impurity phase (refined fraction of 9.58% for the neutron and 5.51% for the x-ray diffraction data) with an orthorhombic lattice. Based on the lattice parameters and the magnetic properties, the composition of this impurity phase was determined to be close to $La_{0.6}Sr_{0.4}MnO_3$. The presence of a La-rich impurity phase implies that the major phase is Sr rich relative to the target composition. However, even if this impurity is taken into account, the x value of our $n=2$ RP phase is 0.305 at most.

Because of the magnetic impurity phase, the refinements of the neutron diffraction data were performed with a four-phase model, both nuclear and magnetic phases for the major $n=2$ RP and the impurity phases. In Figs. 2(a) and 2(b), we show the refinement results for the room-temperature and 15 K data. The atomic positions and selected bond distances obtained for some representative temperatures are listed in Tables II and III, respectively.

The variation of the lattice parameters with temperature is plotted in Fig. 3. Both the a and c parameters decrease with cooling. There is an abrupt contraction of the c parameter by 0.02 Å ($\Delta c/c=0.13\%$) in the temperature range 100–70 K,

TABLE II. Refinements of the neutron diffraction data for $La_{2-2x}Sr_{1+2x}Mn_2O_7$, $x=0.3$, at some selected temperatures.

	15 K	85 K	115 K	300 K
	z/B (Å^2)	z/B (Å^2)	z/B (Å^2)	z/B (Å^2)
O(1)	0/0.30(11)	0/0.47(13)	0/0.73(12)	0/1.06(13)
O(2)	0.1961(2)/0.69(14)	0.1958(3)/1.2(2)	0.1963(2)/1.14(15)	0.1956(2)/1.13(13)
O(3)	0.0959(2)/0.55(6)	0.0955(2)/0.45(7)	0.0956(2)/0.52(7)	0.0955(1)/0.56(6)
La(1)/Sr(1)	0.5/0.08(10)	0.5/0.20(12)	0.5/0.29(11)	0.5/0.25(11)
La(2)/Sr(2)	0.3178(2)/0.31(7)	0.3169(2)/0.29(8)	0.3174(2)/0.31(7)	0.3171(2)/0.39(7)
Mn	0.0958(4)/0.15(10)	0.0973(4)/0.23(11)	0.0968(4)/0.10(10)	0.0971(3)/0.18(10)
M (μ_B)/θ(deg)	3.07(5)/30.5(15)	1.48(9)/40(6)		
a (Å)	3.86493(8)	3.86490(9)	3.86484(8)	3.86920(7)
c (Å)	20.2281(8)	20.2441(9)	20.2584(8)	20.3092(7)
V (Å^3)	302.16(2)	302.40(2)	302.60(2)	304.04(1)
wRp	11.8	11.9	11.3	10.5
Rp	8.62	8.79	8.25	7.68
χ^2	3.99	3.80	3.37	3.20

TABLE III. Selected bond distances and angles for $La_{2-2x}Sr_{1+2x}Mn_2O_7$, $x=0.3$, at some selected temperatures

	15 K	85 K	115 K	300 K
Mn-O(1)	1.938(7)	1.969(8)	1.960(8)	1.971(7)
Mn-O(2)	2.028(9)	1.994(10)	2.018(9)	2.001(8)
Mn-O(3)	1.9325(0)	1.9328(2)	1.9326(1)	1.9349(1)
O(1)-Mn-O(3)	90.1(2)	88.9(3)	89.3(2)	89.0(2)
O(3)-Mn-O(3)	179.893(5)	177.888(9)	178.595(7)	178.063(7)

indicating a magnetostrictive effect, while the *a* parameter shows no such effect. The AF $x=0.3$ sample of Argyriou *et al.* also showed a magnetostrictive contraction of the *c* axis below T_c by 0.14%. Their magnetic structure showed that the Mn spins are aligned along the *c* axis with a tilting angle.[11] On the other hand, the $x=0.4$ compound was reported to show a magnetostrictive effect on the *a* parameter,[12] which appears to be related with the direction of spin orientation as discussed below.

The low-temperature neutron diffraction patterns showed magnetic Bragg peaks below T_c (100 K) (Fig. 4). These are indexed on the nuclear unit cell, and their systematic extinction conditions conform to the space group $I4/mmm$ of the nuclear unit cell, consistent with a long-range FM ordering. In their papers, Argyriou *et al.* and Perring *et al.* reported magnetic peaks such as (001) and (005), which led them to conclude that their compound had AF interbilayer interactions.[10,11] Moreover, Argyriou *et al.* reported that their sample contained a minor FM phase in addition to the major AF phase, consistent with the biphasic nature of their sample revealed from a synchrotron x-ray diffraction. The absence of any AF peaks in our sample indicates that it is a pure ferromagnet.

The variations of some magnetic peak intensities are plotted as a function of temperature in Fig. 5(a). In this figure, we have chosen the (004) and (110) reflections that correspond to the projections onto the *ab* plane and *c* axis, respectively, of the magnetic moment vector. The ratio of these two peaks is related to the tilting angle of the magnetic moment vector from the *c* axis as shown in the following relations:

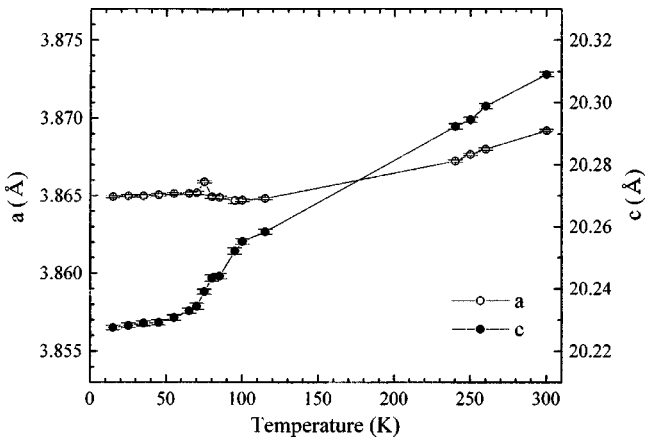

FIG. 3. Temperature variations of lattice parameters of $La_{2-2x}Sr_{1+2x}Mn_2O_7$, $x=0.3$, from powder neutron diffraction pattern refinements

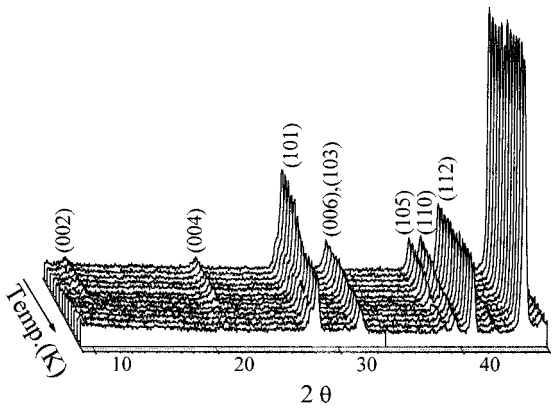

FIG. 4. Temperature variations of the neutron diffraction pattern of $La_{2-2x}Sr_{1+2x}Mn_2O_7$, $x=0.3$.

$$I(004) \propto |M|^2 \sin^2 \theta,$$

$$I(110) \propto |M|^2 \cos^2 \theta,$$

$$I(004)/I(110) = K \tan^2 \theta,$$

where $|M|$ is the amplitude of the magnetic moment vector, θ is the tilting from the *c* axis, and *K* is a constant. As can be seen in the figure, the (004) peak intensity shows a normal behavior, decreasing as the temperature is increased to T_c, while the (110) peak intensity shows an anomalous behavior with temperature, peaking at about 75 K. The resulting tilting angle also reaches its maximum value at 75 K [Fig. 5(b)]. It initially increases from 30° at 15 K to 52° at 75 K, and then drops to 20° at 95 K. Above 95 K, the refinements of the

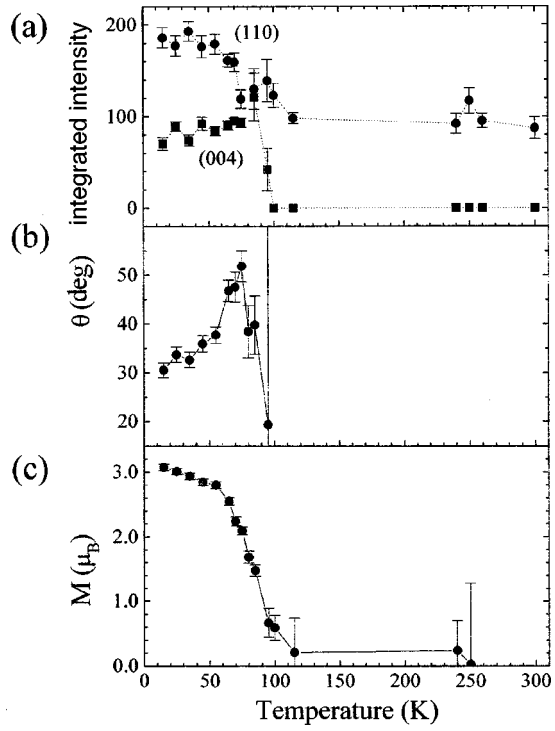

FIG. 5. Temperature variations of the integrated intensities of the (004) and (110) magnetic Bragg peaks (a), refined and tilting angle(θ) (b), magnetic moment (M) (c) of $La_{2-2x}Sr_{1+2x}Mn_2O_7$, $x=0.3$.

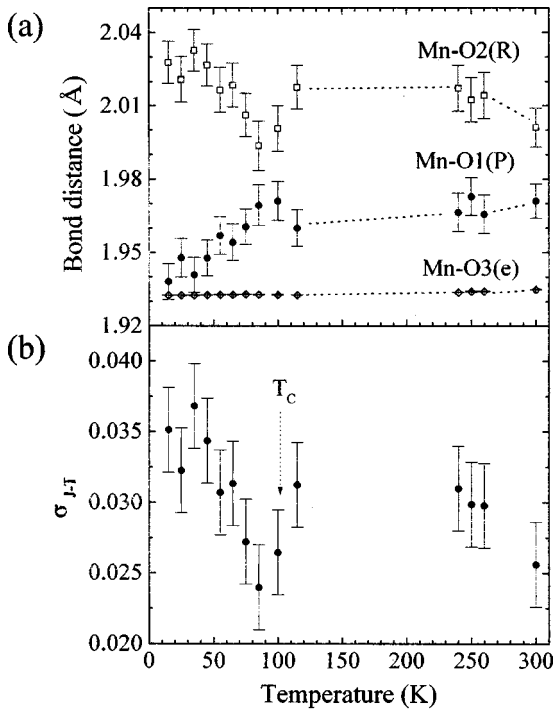

FIG. 6. Temperature variations of Mn-O bond distances (a) and octahedral distortion parameter (b) of $La_{2-2x}Sr_{1+2x}Mn_2O_7$, $x=0.3$, from powder neutron diffraction pattern refinements.

tilting angles resulted in large uncertainties due to the very weak magnetic peak intensities. As mentioned, this behavior of the temperature-dependent tilting angle is anomalous. All of the other $n=2$ RP phases studied by neutron diffraction are reported to show either monotonic changes or no changes of tilting angles with temperature. The temperature range of the tilting angle anomaly coincides with that of the magnetostrictive effect, implying a direct relationship. On the other hand, the refined magnetic moment (M) of the Mn atom decreases monotonically with the increase of temperature from $3.07(5)\mu_B$ at 15 K to zero at around 115 K [Fig. 5(c)]. The magnetic moment value at 15 K is close to the experimental value of $3.2\mu_B$ (under 5000 G), which is close to the theoretical value of $3.7\mu_B$ for a fully aligned Mn moment.[14] This magnetic structure is different from that described for the FM impurity phase of Argyriou *et al.* For the minor FM phase in their sample, Argyriou *et al.* reported AF interactions between the neighboring double layers along the *ab* direction.

In order to understand the complex behavior of the magnetic moment, we refined the crystal structure variation as a function of temperature (Fig. 6 and Table III). At room temperature, the coordination environment of a Mn atom can be described as a tetragonally elongated octahedron with four short equatorial Mn-O(3) bonds (1.9349 Å), one longer Mn-O(2) (2.001 Å), and one intermediate Mn-O(1) (1.971 Å) axial bond. Overall, the MnO_6 octahedron of the $x=0.3$ compound is more distorted than that of the $x=0.4$ one. In the latter, the equatorial Mn-O(3) (1.937 33 Å) and Mn-O(1) (1.942 Å) of the bilayer are close to each other and the Mn-O(2) (1.994 Å) is longer than the others, but with a smaller amount.[12] This difference, of course, is a consequence of a reduced Jahn-Teller distortion because of the lower concentration of Mn^{3+} in the $x=0.4$ compound. While the Mn-O(3) bond distance of our $x=0.3$ compound is almost constant with temperature, showing a slight thermal expansion, the axial Mn-O bond lengths are strongly temperature dependent [Fig. 6(a)]. Between 300 K and T_c (100 K), the Mn-O(1) distance decreased to 1.960 Å, while the Mn-O(2) distance increased to 2.018 Å, making the difference in axial bond lengths even larger. Over the temperature interval 100–75 K these trends are actually reversed and, by 85 K, Mn-O(1) has increased to 1.969 Å and Mn-O(2) has decreased to 1.994 Å, resulting in a much smaller axial bond length difference than at room temperature. From 75 K downwards, the signs of the thermal expansions change again and, at 15 K, Mn-O(1) is much reduced to 1.938 Å and Mn-O(2) is much increased to 2.028 Å. As well, the equatorial Mn-O(3) (1.9325 Å) and axial Mn-O(1) (1.938 Å) distances in the bilayer are not significantly different at 15 K. Therefore, at this temperature, the MnO_6 octahedron can be described as having five short and one long Mn-O long bonds. In comparison, the 11 K data of Argyriou *et al.* give slightly more different values for 1.9551 Å [Mn-O(1)] and 1.929 29 Å [Mn-O(3)].[11]

It is also of interest to compare the temperature variation of the three Mn-O distances of the nominal $x=0.3$ samples, the one described here and that of Ref. 11. As both materials can be regarded as single phase with respect to the neutron diffraction data, such comparisons should be valid. Although only a few details are given in Ref. 11, it is clear that the longer axial bond Mn-O(2) shows a contraction below T_c (100 K) which is barely significant, 2.043(4) Å at 100 K and 2.036(4) Å at 11 K. In the sample reported here, we note an expansion, 2.018(9) Å (115 K) to 2.028(9) Å (15 K), also barely significant, but clearly in the opposite sense to that reported in Ref. 11. In both samples the shorter axial Mn-O(1) bond length decreases with temperature.

It is also a common practice to examine the temperature dependence of a Jahn-Teller distortion index σ_{JT}. This is often defined as a simple ratio $d\langle\text{Mn-O}\rangle_{\text{axial}}/d\langle\text{Mn-O}\rangle_{\text{equatorial}}$. It has been reported that σ_{JT}, so defined decreases with decreasing temperature upon entering the FM regime for $x=0.3$, while an increase occurs for $x=0.4$.[11] The temperature variation of σ_{JT} for our $x=0.3$ sample shows no significant change over the entire temperature range studied. While a very slight decrease upon entering the FM state may be masked by the relatively higher errors on the bond distances from our study, the null result appears to be due, primarily, to the fact that the two axial bond distances have opposite and nearly quantitatively compensating temperature dependences. This observation is consistent with the argument, posed earlier, that our sample is slightly more Sr rich than the sample of Ref. 11; that is, it exhibits behavior intermediate between that reported for the nominal $x=0.3$ and 0.4 phases.

Another type of distortion index has been used:[23]

$$\sigma_{JT}=[\tfrac{1}{6}\Sigma\{(\text{Mn-O})_i\text{-}\langle\text{Mn-O}\rangle\}^2]^{1/2},$$

which is the variance of the Mn-O bond distances and provides a measure of the overall distortion within the Mn-O octahedron. For these materials it is also a measure of the Jahn-Teller distortion as the four equatorial Mn-O distances are equal and thermally invariant, while the axial Mn-O dis-

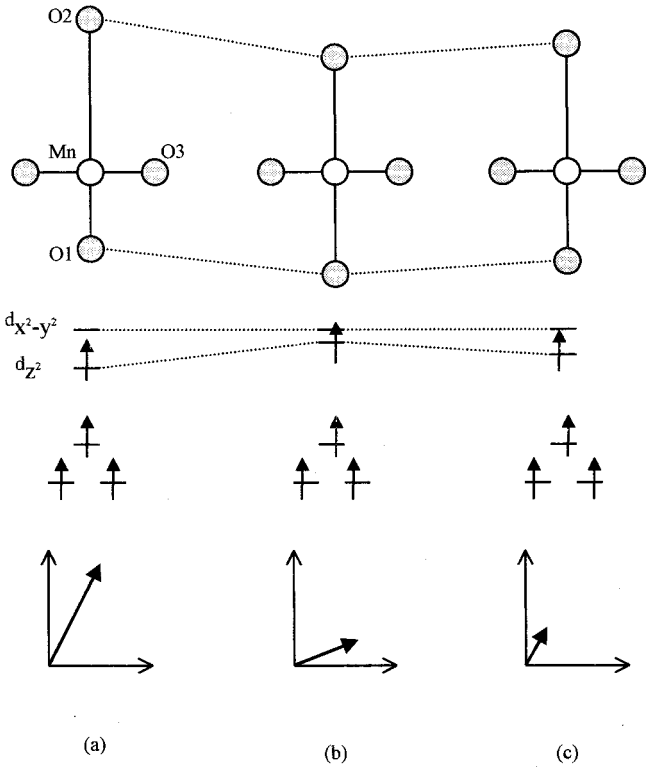

FIG. 7. Schematic diagram for the correlation of the spin direction and crystal-field-split Mn *d* levels derived from the Mn-O bond distances at different temperatures: (a) at 15 K, (b) 85 K, and (c) 100 K.

tances vary strongly with temperature. The thermal variation of this parameter is plotted in Fig. 6(b) and indicates that the distortions are greatest at temperatures above T_c and well below T_c with a pronounced minimum at 85 K.

By comparison of Figs. 5(b) and 6(b) it is clear that the tilt angle of the Mn moment is correlated with the variance-based version of σ_{JT}. This can be understood, qualitatively, by consideration of the effect of the Mn-O environment distortion on the splitting of the Mn *d* levels (Fig. 7). At all temperatures $d(\mathrm{Mn\text{-}O})_{\mathrm{axial}} > d(\mathrm{Mn\text{-}O})_{\mathrm{equatorial}}$, so the d_{z^2} orbital will be stabilized with respect to the $d_{x^2-y^2}$ orbital and in general the preferred moment direction should be parallel to the local *z* axis which is parallel to the crystallographic *c* axis. As for these materials the moment direction is never exactly parallel to *c*, this implies, in the simplest picture, that the crystal field ground state involves a linear combination of d_{z^2} and $d_{x^2-y^2}$. One expects the $d_{x^2-y^2}$ proportion of the admixture to increase as σ_{JT} decreases, which should lead to an increase in the tilt angle, which is in qualitative agreement with observation.

In summary, the sample of $La_{2-2x}Sr_{1+2x}Mn_2O_7$ with nominal $x=0.3$, prepared by a solid-state ceramic method, has been shown by powder neutron diffraction to have a ferromagnetic magnetic structure in which the Mn moments are canted with respect to the *c* axis. The canting angle is strongly temperature dependent and markedly anomalous with values near 20°–30° just below T_c and at low temperatures (15 K) and a maximum of 50° near 75 K. This anomalous temperature behavior can be correlated with changes in the Mn-O bond distances via a Jahn-Teller distortion index and a qualitative crystal field argument.

These results are in contrast to those reported for other nominal $x=0.3$ samples,[10,11] prepared by a floating zone melt method, for which an antiferromagnetic component to the magnetic structure is observed. Otherwise, the two samples show essentially the same bulk magnetic behavior, a T_c of 100 K and a 0.13–0.14 % magnetostrictive effect on the *c*-axis lattice constant. The principal difference appears to be the Sr content or the actual, as opposed to the nominal, *x* value. Comparing unit cell volumes 304.04(1) Å^3 (this work) and 303.43 Å^3 (Ref. 11), it is reasonable to argue that the Sr content or *x* value of the present sample is somewhat greater than that of Ref. 11. It is thus abundantly clear that for the $La_{2-2x}Sr_{1-2x}Mn_2O_7$ system, near $x=0.3$, the details of the magnetic structure are remarkably sensitive to small variations in *x*.

ACKNOWLEDGMENTS

Financial support for this research from the Korea Science and Engineering Foundation (Grant No. KOSEF 971-0305-050-3, Y.-U.K.) and Natural Science and Engineering Research of Canada (NSERC, J.E.G.) is gratefully acknowledged. The neutron diffraction experiment has been performed at HRPD operated under a nuclear *R&D* program by MOST.

[1] Y. Moritomo, A. Asamitsu, J. Kuwahara, and Y. Tokura, Nature (London) **380**, 141 (1996).
[2] T. Kimura, Y. Tomioka, H. Kuwahara, A. Asamitsu, M. Tamura, and Y. Tokura, Science **274**, 1698 (1996).
[3] R. Mahesh, R. Mahendiran, A. K. Cheetham, and C. N. R. Rao, J. Solid State Chem. **122**, 448 (1996).
[4] D. Louca, G. H. Kwei, and J. F. Mitchell, Phys. Rev. Lett. **80**, 3811 (1998).
[5] T. Kimura, A. Asamitsu, Y. Tomioka, and Y. Tokura, Phys. Rev. Lett. **79**, 3720 (1997).
[6] D. N. Argyriou, T. M. Kelley, J. F. Mitchell, R. A. Robinson, R. Osborn, S. Rosenkranz, R. I. Sheldon, and J. D. Jorgensen, J. Appl. Phys. **83**, 6374 (1998).
[7] C. D. Potter, M. Swiatek, S. D. Bader, D. N. Argyriou, J. F. Mitchell, D. J. Miler, D. G. Hinks, and J. D. Jorgensen, Phys. Rev. B **57**, 72 (1998).
[8] S. D. Bader, R. M. Osgood, III, D. J. Miller, J. F. Mitchell, and J. S. Jiang, J. Appl. Phys. **83**, 6385 (1998).
[9] R. H. Heffner, D. E. MacLaughlin, G. J. Nieuwenhuys, T. Kimura, G. M. Luke, Y. Tokura, and Y. J. Uemura, Phys. Rev. Lett. **81**, 1706 (1998).
[10] T. G. Perring, G. Aeppli, T. Kimura, Y. Tokura, and M. A. Adams, Phys. Rev. B **58**, R14 693 (1998).
[11] D. N. Argyriou, J. F. Mitchell, P. G. Radaelli, H. N. Bordallo, D. E. Cox, M. Medarde, and J. D. Jorgensen, Phys. Rev. B **59**, 8695 (1999).
[12] J. F. Mitchell, D. N. Argyriou, J. D. Jorgensen, D. G. Hinks, C. D. Potter, and S. D. Bader, Phys. Rev. B **55**, 63 (1997).

[13] D. N. Argyriou, J. F. Mitchell, C. D. Potter, S. D. Bader, R. Kleb, and J. D. Jorgensen, Phys. Rev. B **55**, R11 965 (1997).
[14] N. H. Hur, J.-T. Kim, K. H. Yoo, Y. K. Park, J. C. Park, E.-O. Chi, and Y.-U. Kwon, Phys. Rev. B **57**, 10 740 (1998).
[15] A. Urushibara, Y. Moritomo, T. Arima, A. Asamitsu, G. Kido, and Y. Tokura, Phys. Rev. B **51**, 14 103 (1995).
[16] J. Rodriguez-Carvajal, computer program FULLPROF, Version 3.2 Jan97-LLB-JRC, Laboratoire Leon Brillouin, CEA-CNRS, 1997.
[17] A. C. Larson and R. B. Von Dreele, LANSCE, MS-H805, Los Alamos National Laboratory, Los Alamos, NM, 1985–1994.
[18] P. D. Battle, M. A. Green, N. S. Laskey, J. E. Millburn, L. Murphy, M. J. Rosseinsky, S. P. Sullivan, and J. F. Vente, Chem. Mater. **9**, 552 (1997).
[19] R. Seshadri, C. Martin, A. Maignan, M. Hervieu, B. Raveau, and C. N. R. Rao, J. Mater. Chem. **6**, 1585 (1996).
[20] R. Shshadri, C. Martin, M. Hervieu, B. Raneau, and C. N. R. Rao, Chem. Mater. **9**, 270 (1997).
[21] P. D. Battle, M. A. Green, N. S. Laskey, J. E. Millburn, P. G. Radaelli, M. J. Rosseinsky, S. P. Sullivan, and J. F. Vente, Phys. Rev. B **54**, 15 967 (1996).
[22] P. D. Battle, J. A. Hepburn, J. E. Milburn, P. G. Radaelli, M. J. Rosseinsky, L. E. Spring, and J. F. Vente, Chem. Mater. **9**, 3215 (1997).
[23] P. G. Radaelli, G. Iannone, M. Marezio, H. Y. Hwang, S.-W. Cheong, J. D. Jorgensen, and D. N. Argyriou, Phys. Rev. B **56**, 8265 (1997).